MEASUREMENT OF MASS DEPENDENCE OF THE TRANSVERSE MOMENTUM OF LEPTON PAIRS IN DRELL–YAN PRODUCTION AT $\sqrt{s} = 13$ TeV*

Kyeongpil Lee

on behalf of the CMS Collaboration

Université Libre de Bruxelles, Belgium

Received 30 November 2022, accepted 23 January 2023, published online 25 May 2023

A measurement of the differential Drell–Yan cross section in the di-electron and dimuon channel is presented with respect to the transverse momentum of the dilepton pair $p_{\mathrm{T}}(\ell\ell)$ in the several dilepton mass ranges from 50 GeV to 1 TeV. The result is based on the proton–proton collision data at $\sqrt{s} = 13$ TeV recorded with the CMS detector at the LHC. The corresponding integrated luminosity is 36.3 fb^{-1}. Additional measurements are also performed including the cross section as a function of φ^*_η which is correlated to $p_{\mathrm{T}}(\ell\ell)$, the cross section with at least one jet in the final state, and the cross-section ratio with respect to the result in the Z mass peak region. Various comparisons to the latest theoretical predictions are presented with different approaches based on quantum chromodynamics including soft-gluon resummation.

DOI:10.5506/APhysPolBSupp.16.5-A34

1. Introduction

The Drell–Yan (DY) process is the process with two charged lepton pairs in the final state produced via Z or virtual photon exchange. The measurement of the transverse momentum of the DY pair ($p_{\mathrm{T}}(\ell\ell)$) can provide various and useful information for understanding of the soft and hard radiation in quantum chromodynamics (QCD) depending on the regime. In the low $p_{\mathrm{T}}(\ell\ell)$ region, the resummation of the soft gluon radiation is necessary to properly describe the $p_{\mathrm{T}}(\ell\ell)$ distribution. Moreover, this region is sensitive to the effect of the intrinsic transverse momentum of the colliding partons, which is described by the transverse-momentum-dependent (TMD) parton distribution function (PDF) approach. On the other hand, the high-$p_{\mathrm{T}}(\ell\ell)$

* Presented at the Diffraction and Low-x 2022 Workshop, Corigliano Calabro, Italy, 24–30 September, 2022.

region is dominated by the effect of the fixed-order perturbative QCD. Therefore, by measuring the $p_{\mathrm{T}}(\ell\ell)$ spectrum, the validity of various theoretical approaches can be tested, and it can be used as an important constraint for their development. In addition, measurements in different dilepton mass ($m_{\ell\ell}$) range can test and constrain the scale evolution of the theoretical approaches as well.

The other measurement of φ^*_η can provide complementary information on the $p_{\mathrm{T}}(\ell\ell)$ spectrum. φ^*_η is defined in Eq. (1), where $\Delta\varphi$ is the difference of the azimuthal angles of two leptons and θ^*_η can be expressed in terms of the pseudo-rapidity of charged leptons ($\eta^{\pm}$), as $\cos(\theta^*_\eta) = \tanh[(\eta^+ - \eta^-)/2]$,

$$\varphi^*_\eta \equiv \tan\left(\frac{\pi - \Delta\varphi}{2}\right)\sin(\theta^*_\eta)\,. \tag{1}$$

According to the definition, it depends on the angular variables only, which can precisely be measured compared to $p_{\mathrm{T}}(\ell\ell)$. As φ^*_η is known to be related to $p_{\mathrm{T}}(\ell\ell)/m_{\ell\ell}$, the measurement of φ^*_η can be used as an indirect measurement of $p_{\mathrm{T}}(\ell\ell)$ with high precision.

This article presents the differential DY cross-section measurement in the dimuon and dielectron channel with respect to $p_{\mathrm{T}}(\ell\ell)$ and φ^*_η in different $m_{\ell\ell}$ ranges from 50 GeV to 1 TeV. The $p_{\mathrm{T}}(\ell\ell)$ spectrum is also measured in events with at least one jet in the final state. The measurement is based on the proton–proton collision data collected with the CMS detector [1] at the CERN LHC, and the corresponding integrated luminosity is 36.3 fb^{-1}.

Several complementary measurements for the DY process have been performed at the same center-of-mass energy by ATLAS, CMS, and LHCb collaborations [2–6].

2. Event selection and background estimation

As a first step of the measurement, several conditions are applied to the events to select DY pair candidates with small background contamination. In the dimuon channel, the data samples collected with isolated single and double muon triggers are used. The isolated double electron trigger is used for the dielectron channel. In both channels, the transverse momentum (p_{T}) of the leading (sub-leading) lepton should be larger than 25 (20) GeV, and the absolute value of η is restricted to values smaller than 2.4. Standard identification criteria and isolation requirements are applied to both muons and electrons. Veto on the events with the third lepton or b jets is used to suppress the backgrounds. Additionally, for the measurement with at least one jet, jets are reconstructed with the anti-k_{T} algorithm with $\Delta R = 0.4$. Jets with $p_{\mathrm{T}} > 30$ GeV and $|\eta| < 2.4$ are selected. ΔR between lepton and jet should be larger than 0.4 to avoid the overlap between them.

After the event selection, the remaining backgrounds are estimated and subtracted from the data. Most of them are estimated using the MC simulation which includes top-quark (top-quark pair and single top), $Z/\gamma^* \to \tau\tau$, diboson (WW, WZ, and ZZ), and photon-induced processes. Small backgrounds from misidentified leptons are estimated using the data control sample with the same sign. This background is estimated in the dielectron channel only where the contribution is non-negligible. After the estimation, the data and the prediction shows good agreement in general over the entire mass range in both channels.

3. Unfolding and combination

After the background subtraction, unfolding correction is applied to the data yield to correct the migration effect between measurement bins due to the detector resolution. The response matrix is obtained from the MC simulation for the DY process generated by the aMC@NLO generator [7, 8]. The target phase space for the unfolding is defined as follows. The p_{T} of the leading (sub-leading) lepton should be larger than 25 (20) GeV with $|\eta| < 2.4$. The momenta of the leptons are corrected by adding the momentum of photons near the lepton with $\Delta R < 0.1$ (dressed lepton). For the jets, $p_{\mathrm{T}} > 30$ GeV and $|\eta| < 2.4$ is required. Additionally, jets should be separated from the leptons by the condition $\Delta R > 0.4$ between leptons and jets. The unfolding correction is applied using D'Agostini's iterative method [9] with early stopping.

After the unfolding correction, the results from dimuon and dielectron channels are transformed into a common phase space, and the combination is performed to have better precision. The central value is obtained by the weighted mean of the two channels according to the inverse of associated uncertainties. The uncertainty of the combined result is estimated by propagating the uncertainties from individual channels with each covariance matrix. The details on the combination method can be found in [10]. For the highest mass bin (350 GeV $< m_{\ell\ell} <$ 1000 GeV), only the dielectron channel is used due to the insufficient resolution of the result from the muon channel.

4. Systematic uncertainties

For the inclusive DY measurement, the total uncertainty is about 2–3% in general, except for the high mass and p_{T} region where the statistics is small. The total uncertainty goes down to about 1% in the case of the cross-section ratio with respect to the results at the Z peak region due to the cancellation of partial systematic uncertainties. The dominant uncertainty is the luminosity uncertainty with the size of about 1.2%, followed by the

uncertainty from the efficiency correction. The statistical uncertainty from data and MC becomes dominant in the high mass and p_{T} region. For the measurement with at least one jet, the overall uncertainty level is about 10%, which is mostly coming from the jet energy and scale correction.

5. Results

The differential DY cross sections with respect to $p_{\mathrm{T}}(\ell\ell)$ after the combination are compared to the various theoretical predictions. Figure 1 shows the prediction over data ratio in various mass ranges. The predictions are based on the matrix element combined with the parton shower. The prediction used in the left plot is generated by the aMC@NLO generator, and it is merged with PYTHIA 8 [11] for the parton shower. It shows generally good agreement over the entire mass range, except for the low-$p_{\mathrm{T}}(\ell\ell)$ region. This low-$p_{\mathrm{T}}(\ell\ell)$ region is sensitive to the choice of the tune parameter, but the associated uncertainty is not included in the prediction. On the other hand, the prediction in the right plot is based on the MiNNLO$_{\mathrm{PS}}$ approach [12] at the accuracy of next-to-next-to-leading order (NNLO) with the parton shower by PYTHIA 8. The high $p_{\mathrm{T}}(\ell\ell)$ region is well described due to its high order perturbative QCD correction, and it is also successful in the low $p_{\mathrm{T}}(\ell\ell)$ as well due to the modified tune parameter. It shows the best agreement with the data among the predictions presented in this article.

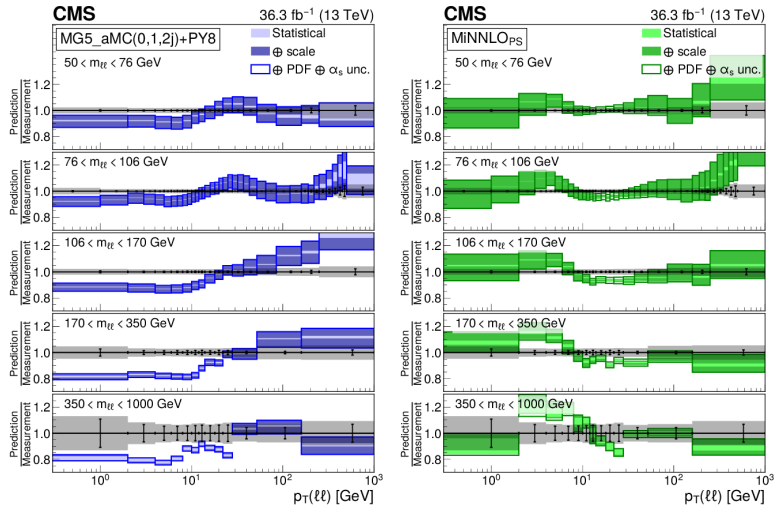

Fig. 1. Prediction-to-data ratio of the differential cross sections as a function of $p_{\mathrm{T}}(\ell\ell)$ in various mass ranges. Left: Comparison to MC prediction from aMC@NLO + parton shower. Right: Comparison to MC prediction from MiNNLO$_{\mathrm{PS}}$ + parton shower.

Another comparison is presented in Fig. 2. The left plot shows the comparison to the theoretical prediction with parton branching TMD from CASCADE [13]. The matrix element is calculated using the Madgraph generator. Parton shower is done with PYTHIA 6. It shows good agreement in the low-$p_{\mathrm{T}}(\ell\ell)$ region even though the PDF is extracted from the independent measurements from HERA. It fails to describe the high-$p_{\mathrm{T}}(\ell\ell)$ region due to the missing higher-order QCD correction. The prediction in the middle plot is the analytical prediction from ArTeMiDe based on the TMD as well. It has a limited validity range in $p_{\mathrm{T}}(\ell\ell) < 0.2 m_{\ell\ell}$. Within its validity range, it has remarkable agreement with the data near the Z peak region because the TMD is extracted from the previous LHC measurements of Z events. However, it also shows good agreement in the other mass range, indicating the validity of scale evolution. The last comparison in the right plot is the results based on GENEVA-q_{T} MC generator with NNLO accuracy and high order resummation in q_{T}. Except for the discrepancy in the middle-$p_{\mathrm{T}}(\ell\ell)$ region and in the lowest-$m_{\ell\ell}$ region, it generally shows good agreement.

The full results including the φ^*_η results, cross-section ratio, and cross sections with at least one jet can be found in [14].

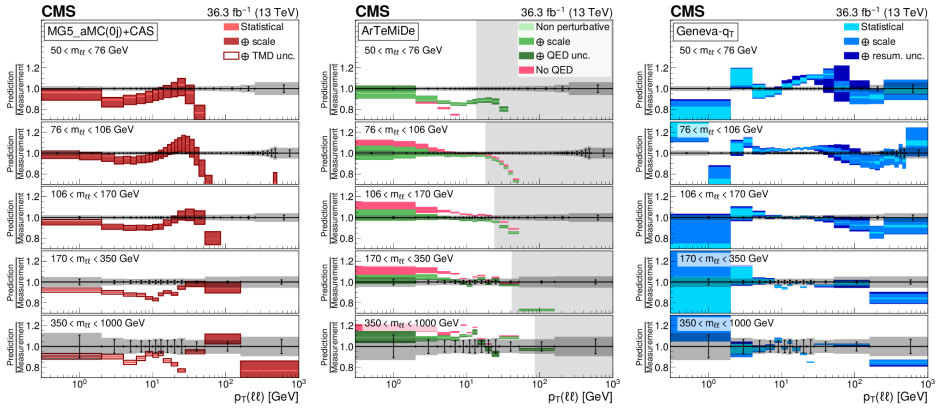

Fig. 2. Prediction-to-data ratio of the differential cross sections as a function of $p_{\mathrm{T}}(\ell\ell)$ in various mass ranges. Left: Comparison to MC prediction from aMC@NLO with parton branching TMD (CASCADE). Middle: Comparison to the analytic prediction from ArTeMiDe. Right: Comparison to the GENEVA-q_{T} prediction.

6. Summary

The differential DY cross section as a function of $p_{\mathrm{T}}(\ell\ell)$ is presented based on the proton–proton collision data collected with the CMS detector at the LHC, corresponding to the integrated luminosity of 36.3 fb^{-1}. The overall precision is about 2–3%, and the results are compared to various theoretical predictions. The details can be found in [14].

REFERENCES

[1] CMS Collaboration (S. Chatrchyan *et al.*), *J. Instrum.* **3**, S08004 (2008).

[2] CMS Collaboration (A.M. Sirunyan *et al.*), *J. High Energy Phys.* **2019**, 059 (2019).

[3] CMS Collaboration (A.M. Sirunyan *et al.*), *J. High Energy Phys.* **2019**, 061 (2019).

[4] CMS Collaboration (A.M. Sirunyan *et al.*), *J. High Energy Phys.* **2020**, 076 (2020).

[5] ATLAS Collaboration (G. Aad *et al.*), *Eur. Phys. J. C* **80**, 616 (2020).

[6] LHCb Collaboration (R. Aaij *et al.*), *J. High Energy Phys.* **2016**, 136 (2016).

[7] J. Alwall *et al.*, *J. High Energy Phys.* **2014**, 079 (2014).

[8] R. Frederix, S. Frixione, *J. High Energy Phys.* **2012**, 061 (2012).

[9] G. D'Agostini, *Nucl. Instrum. Methods Phys. Res. A* **362**, 487 (1995).

[10] CMS Collaboration (V. Khachatryan *et al.*), *J. High Energy Phys.* **2017**, 022 (2017).

[11] T. Sjöstrand *et al.*, *Comput. Phys. Commun.* **191**, 159 (2015).

[12] P.F. Monni *et al.*, *J. High Energy Phys.* **2020**, 143 (2020).

[13] S. Baranov *et al.*, *Eur. Phys. J. C* **81**, 425 (2021).

[14] CMS Collaboration, «Measurement of the mass dependence of the transverse momentum of lepton pairs in Drell–Yan production in proton–proton collisions at $\sqrt{s} = 13$ TeV», Technical report, 2022, submitted to *Eur. Phys. J. C*; all figures and tables can be found at `http://cms-results.web.cern.ch/cms-results/public-results/publications/SMP-20-003` (CMS Public Pages).